Supporting Information for

Magnitude of diffusion- and transverse dispersion-induced isotope fractionation of organic compounds in aqueous systems

Fengchao Sun[†, ‡], Jan Peters [†§], Martin Thullner [¶], Olaf A. Cirpka [§], and Martin Elsner[*, †, ‡]

[†]Institute of Groundwater Ecology, Helmholtz Zentrum München, Ingolstädter Landstrasse 1, 85764 Neuherberg, Germany

[‡]Chair of Analytical Chemistry and Water Chemistry, Technical University of Munich, Marchioninistrasse 17, 81377 Munich, Germany

[¶]Department of Environmental Microbiology, UFZ—Helmholtz Centre for Environmental Research, Permoserstrasse. 15, 30418 Leipzig, Germany

[§]Center for Applied Geoscience, University of Tübingen, Schnarrenbergstr. 94-96, 72076 Tübingen, Germany

SUMMARY

18 pages, 4 figures and 5 tables

CONTENTS

Supporting Environmental Section

Chemicals

The following chemicals were used: benzene, toluene and ethylbenzene from Riedel-de Haën, supplied by Sigma Aldrich, Germany, 2,6-dichlorobenzamide (Sigma Aldrich, Germany), s-metolachlor (Chemos GmbH &Co. KG, Germany), potassium chloride (Sigma Aldrich, Germany), uranine (Sigma Aldrich, Germany), and sodium hydroxide (Sigma Aldrich, Germany).

Setup of the two-dimensional flow-through sediment tank experiment

The setup of the two-dimensional (2D) flow-through sediment tank experiment (Figure S1) was adapted from Bauer et al[1]. The tank was built with two glass sheets fitted into the frame made of teflon and aluminum and had the dimensions of 0.955 m × 0.185 m × 0.012 m (L × H × W); the small width of the tank simplified the flow-through system to be two-dimensional. Sixteen inlet and outlet ports were vertically distributed along the left-hand and the right-hand boundaries of the tank with a 1 cm vertical distance between each port. Two peristaltic pumps (Ismatec, Germany) with the same pumping rate (45 ± 2 µL/min per port) at the inlet and outlet boundaries established constant and homogeneous flow conditions within the flow-through tank system. Pumping rates of the pumps with a maximum standard deviation of 8% were calibrated before the experiments. The inlet and outlet ports consisted of stainless steel capillaries (1/16 inch, Alltech, USA) that penetrated the Teflon at the sides of the 2D tank which were connected at the outer side with Viton pump-tubes (ID: 1.02 mm; Ismatec, Glattbrugg, CH) of the peristaltic pumps. At the outlet each steel capillary was in addition covered by steel wire gauze inside the tank to prevent blockage by sands. The tank was sterilized with 12 g/L NaOH solution and rinsed with autoclaved ultra-pure MQ water before each experiment. Autoclaved sands (diameter 0.8-1.2 mm in the BAM

and metolachlor experiment, diameter 0.4-0.8mm in the toluene experiment, MKK Märkische Kies- und Kalksandsteinwerke GmbH, Germany) were homogeneously wet packed into the tank. A solution containing the target compounds (BAM 400 mg/L, metolachlor 100 mg/L and toluene 34.2 mg/l) at natural isotopic abundance was introduced through the central inlet port (z = 8 cm) of the tank, and the medium solution was pumped in through the rest of the inlet ports. Sampling of BAM and metolachlor were assessed by collecting samples from the 16 outlet ports; sampling of toluene was carried out with a syringe pump (Ismatec, Germany). Sampling for the isotope measurements started when steady-state conditions had been established. For BAM and metolachlor sampling was conducted from day 5 to day 20; for toluene sampling was conducted from day 5 to day 8.

Sample preparation and solid-phase extraction (SPE)

Samples from tank experiments were frozen at -20 °C immediately after each sampling until enough sample volume was collected for isotope analysis. For carbon and nitrogen isotope measurements of BAM and metolachlor samples from diffusion cell experiments (40 mL) and tank experiments (1 L) were first filtered through 0.2 μM PES filter (Nalgene Thermo Scientific, Germany) and then were concentrated by SPE.

The SPE method was adapted from Torrentó et al[2]. 0.2 g hydrophobic polymer-based sorbent Bakerbond SDB-1 (J.T. Baker, USA) was self-packed in the 6 mL empty PP SPE cartridge with PE frit (20 μm pore size; Sigma Aldrich, Germany). The SPE steps are illustrated in the figure below.

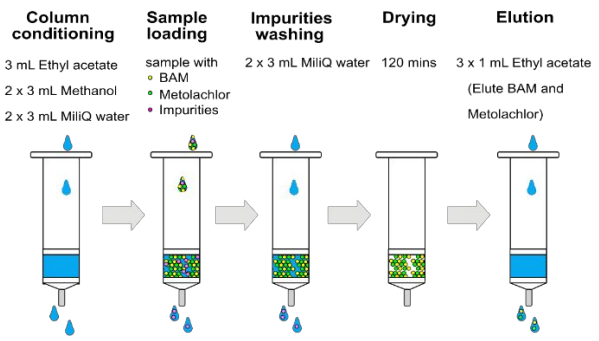

Figure 1 SPE steps

Concentration measurements on HPLC-UV-DAD

BAM and metolachlor concentrations were measured on Prominence HPLC (Shimadzu Corp., Japan) with a 75 × 4.6 mm Kinetex 2.6µm C18 100 Å column and a SecurityGuard ULTRA cartridge for C18 UHPLC (both from Phenomenex Inc., Golden, CO). The volume of injected sample was 50 µL. Separation was performed with a binary gradient flow rate of 1 mL/min at 40 °C. The mobile phase A was a 5 mM KH_2PO_4 (pH 7) buffer solution and the mobile phase B was pure acetonitrile. The initial mobile phase composition was 90% A and 10% B with a 4 min gradient ending with a composition of 70% A and 30% B, followed by a 4 min gradient ending with a composition of 22% A and 78% B. This composition was held for 2 min thereafter returning to the initial conditions in 0.5 min. BAM was detected with UV absorbance at 201 nm, and metolachlor was detected with UV absorbance at 215 nm. All peaks were quantified by LabSolutions V 5.71 SP2 (Shimadzu Corp., Japan).

Concentration measurements on GC-MS

The method of concentration measurements of volatile organic compounds on GC-MS was adapted from Anneser et al.[3] Concentrations of benzene, toluene and ethylbenzene were measured on a Trace DSQ GC-MS system (Thermo Electron, Germany) equipped with a Combi PAL

autosampler (CTC Analytics, Switzerland). A DB-5 analytical column (30 m, 0.25 mm i.d., 0.5 μm film, Agilent Technologies, Germany) with carrier gas He at a flow rate of 1 mL/min was used for separation. 250 μL gas sample were injected at a split ratio of 1:10 in the headspace measurement. The oven temperature started at 80 °C, where it was held for 1 min, then increased to 140 °C at a rate of 15 °C/min, then increased to a final temperature of 220 °C at a rate of 25 °C/min and held for 1.8 min. The MS was operated in the selected ion monitoring mode (SIM). Internal standards of fluorobenzene and 1,4-dichlorobenzene (EPA 524 internal Standard Mix, Supelco, Bellefonte, PA) were added to the samples and standards.

Carbon and nitrogen isotope measurements on GC-IRMS

For the carbon and nitrogen isotope measurements, the samples concentrated in ethyl acetate after SPE were measured on a GC-IRMS system in which a TRACE GC Ultra gas chromatograph (Thermo Fisher Scientific, Italy) was coupled to a Finnigan MAT 253 isotope ratio mass spectrometer (IRMS) through a Finnigan GC Combustion III interface (Thermo Fisher Scientific, Germany). In addition, for carbon isotope measurements of benzene, toluene and ethylbenzene, a Velocity XPT purge and trap sample concentrator with an AQUATek 70 liquid autosampler (Teledyne Tekmar) was connected before the gas chromatograph. The IRMS was operated with a vacuum in the ion source of 2.1×10^6 mbar, an accelerating potential of 9 kV and an emission energy of 1.5 mA for carbon isotope analysis and 2 mA for nitrogen analysis. A DB-5 analytical column (30 m, 0.25 mm i.d., 0.5 μm film, Agilent Technologies, Germany) was used in the gas chromatograph for separation. Helium (grade 5.0) was used as the carrier gas. Samples were injected using a GC Pal autosampler (CTC, Switzerland). For the measurements of high concentrations of BAM and metolachlor the Thermo injector in the split/split-less injection mode was used; for the measurements of BAM and metolachlor at low concentrations and the

measurements of benzene, toluene and ethylbenzene, a programmable injector controlled by an Optic 3 system with liquid N_2-cyofocusing (ATAS GL, distributed by Axel Semrau, Germany) was used. BAM and metolachlor at low concentrations were measured in the on-column injection mode in which a Rxi retention gap (fused silica, 3 m × 0.53 mm inner diameter) (RESTEK, Germany) was connected to a custom made on-column liner, whereas benzene, toluene and ethylbenzene were measured after purge and trap by cryofocusing in a split injection liner.

Vienna PeeDee Belemnite (V-PDB) and Air-N_2 were applied to determine the carbon isotope values $\delta^{13}C$ [‰] and nitrogen isotope values $\delta^{15}N$ [‰] of the samples. The carbon and nitrogen isotope values $\delta^{13}C$ and $\delta^{15}N$ of the samples were calculated in relation to a lab reference gas (CO_2 and N_2, respectively) which was measured against V-PDB and air in the beginning and the end of each run by using international reference materials (provided by IAEA), e.g. the CO_2 gases RM 8562, RM8563 for CO_2, and RM 8564 and NSVEC (N_2) for N_2.

For the measurements of BAM and metolachlor in the split/split-less injection mode, the GC method for BAM and metolachlor started at 80 °C, and then increased to a final temperature of 280 °C at a ramp rate of 15 °C/min, after which the temperature was held for 7 min. A constant flow rate of 1.4 mL/min was maintained during the measurement. The method of on-column injection was adapted from Ehrl et al.[4] The GC oven started at 35 °C, was held for 30 s, and then increased to 80 °C at a ramp rate of 5 °C/min to allow a complete solvent evaporation and compound transfer from the retention gap to the analytical column. Then the temperature increased from 80 °C to 280 °C at a ramp rate of 15 °C/min. The method in the Optic 3 started at an initial temperature of 40 °C, which was held for 300 s and then increased to 250 °C at a ramp rate of 2 °C/s. The column flow rate started from 0.3 mL/min, which was held for 120 s and then increased

to 1.4 mL/min within 2 min. Thus, a stable flow rate of 1.4 mL/min was established before the GC temperature program started.

The method for carbon isotope analysis of benzene, toluene and ethylbenzene on the GC-IRMS was adapted from Qiu et al.[5] The GC oven temperature started at 50 °C, was held for 120 s, and was then increased to 150 °C at a ramp rate of 10 °C/min, where it was held for 1min. Then the temperature increased with a second ramp rate of 100 °C/min to 250 °C, where it was held for 13 min. The method in the Optic 3 started at an initial temperature -80 °C, where it was held for 10 s, then it was increased to 250 °C at a ramp rate of 10 °C/s. The flow rate was kept constant at 1.4 mL/min.

Tracer test with uranine

To determine the properties of the flow system and to validate the numerical simulation of solute transport, we conducted tracer tests with uranine before the transport experiments. For the tracer test before the experiment with BAM and metolachlor, a 30 µg/L uranine solution was continuously injected into the middle inlet port (z = 8 cm) of the tank, at a constant pumping rate of 45 ± 2 µL/min/port. For the tracer test before the experiment with toluene, the pumping rate was 44 ± 2 µL/min/port. The concentration of uranine was measured at the outlets. **Figure 2** shows the vertical distribution curve and the breakthrough curve of the measured outlet-to-inlet concentration ratio of uranine $C_{\mathrm{out}}/C_{\mathrm{in}}$. The measured results were fitted by the numerical simulation. The determined seepage velocity, and longitudinal and transverse dispersivity can be found in the **Table** .

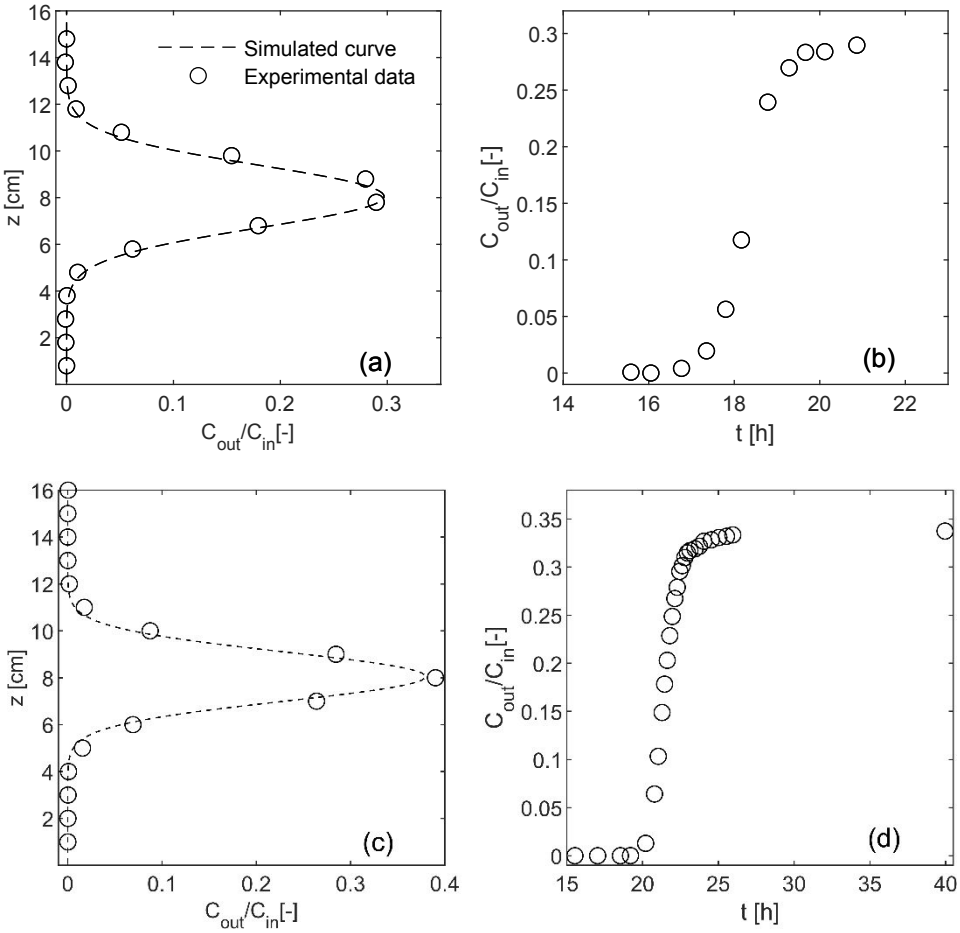

Figure 2 Tracer test results for the continuous injection of uranine before the flow-through tank experiments with (a)-(b) BAM and *s*-metolachlor, and (c)-(d) with toluene: (a), (c) vertical concentration distribution along the outlet profile; (b), (d) breakthrough of uranine at the central outlet port located at z = 8 cm .

Supporting Figures

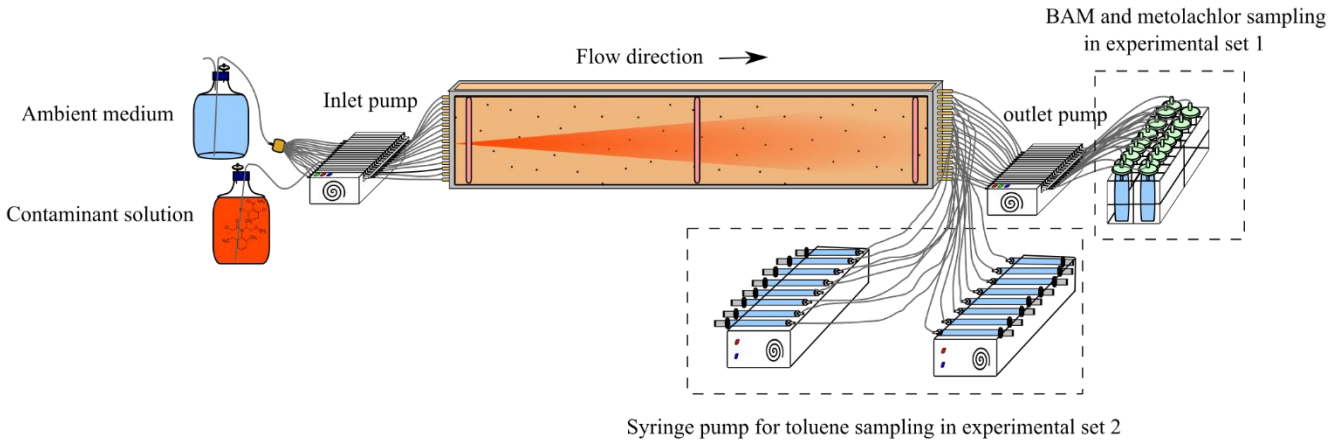

Figure S1 Setup of the two-dimensional flow-through sediment tank experiment

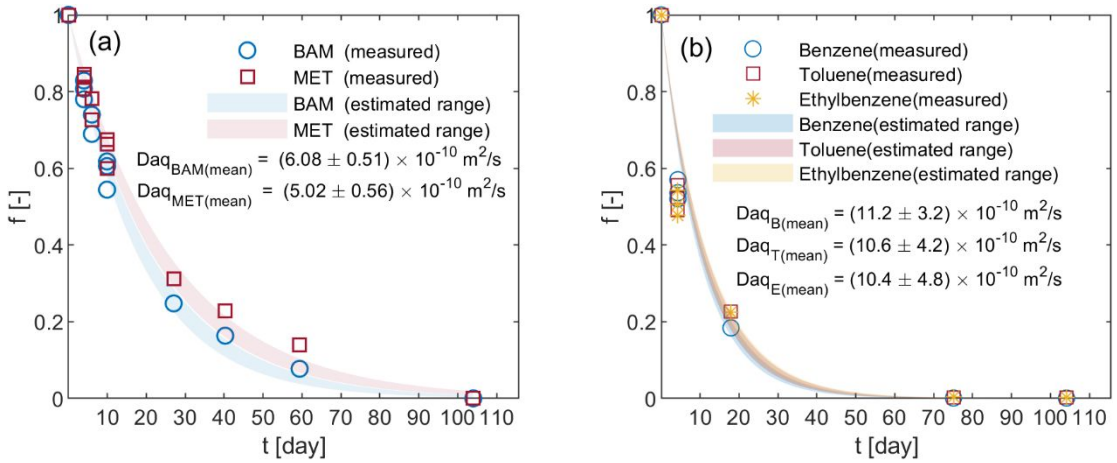

Figure S2 Concentration change with increasing duration in the diffusion cell experiments of (a) BAM and metolachlor (MET) and (b) benzene, toluene and ethylbenzene

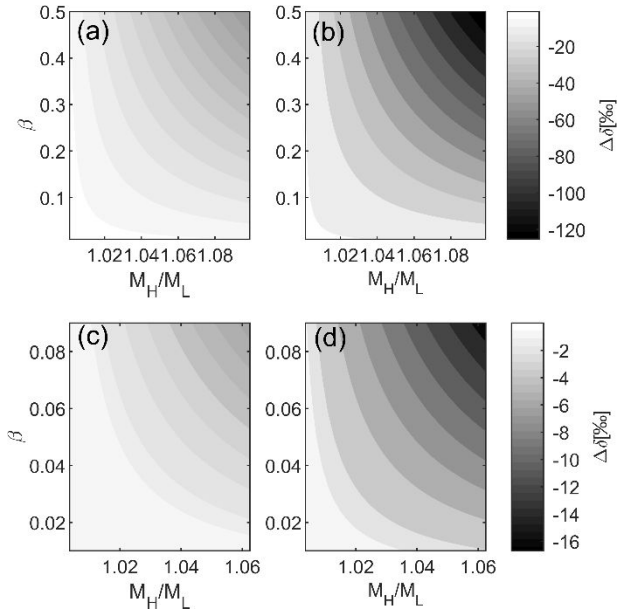

Figure S3 Dependence of $\Delta\delta$ induced by transverse dispersion on the β-value and the ratio between molecular mass of heavy to light isotopologues $M_{\mathrm{H}}/M_{\mathrm{L}}$. $\Delta\delta$ was the maximum isotope fractionation at the lowest concentration site along the vertical outlet profile of the tank system. Panel (a, b): simulations for a test range of β = (0.01– 0.5) and $M_{\mathrm{H}}/M_{\mathrm{L}}$ = (1.001–1.099) by using classical equation and Chiogna et al. equation, respectively; panel (c, d): simulations for organic compounds at natural isotopic abundance for a test range of β = (0.01–0.09) and $M_{\mathrm{H}}/M_{\mathrm{L}}$ = (1.004–1.063) by using classical equation and Chiogna et al. equation, respectively. The lightest regions in the contour plots represent absolute $\Delta\delta$-values smaller than 1‰. The initial isotope ratio $^{13}C/^{12}C$ was arbitrarily set to be 0.0108.

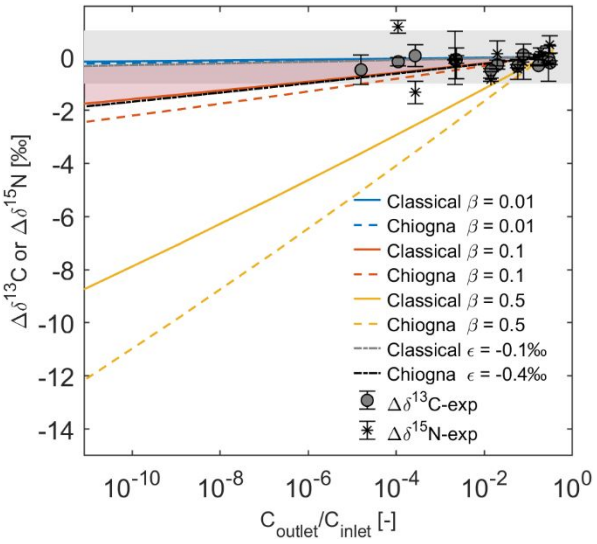

Figure S4. Simulated isotope fractionations $\Delta\delta^{13}$C or $\Delta\delta^{15}$N induced by transverse dispersion at different outlet-to-inlet concentration ratios $C_{\text{outlet}}/C_{\text{inlet}}$ using different β-values and ε-values. Solid lines: with classical linear parameterization of transverse dispersion; dashed lines: with nonlinear parameterization by Chiogna et al.; dotted-dashed lines: nonlinear parameterization by Chiogna et al. with ε = -0.1 and -0.4‰. We used light and heavy isotopologues of BAM (M_{H} = 190.02 Da, M_L = 191.02 Da) as the target compounds, with D_L= 6.08 × 10^{-10} m^2/s. Both dispersion scenarios with the transverse dispersion coefficient D_t =1.5 × 10^{-9} m^2/s. Gray zone represents the ±1‰ tolerated standard deviation of the original standard isotope value. Red zone represents the isotope fractionation range predicted by using Chiogna et al. equation with ε = -0.1 and -0.4‰.

Supporting Tables

Table S1 Initial and final concentrations and calculated remaining fraction and diffusion coefficient of each compound in each diffusion cell experiment running for a different time period

Compound	$C(0)$ [mg/L]	$C(t)$ [mg/L]	f [-]	t [day]	σ [m^{-2}]	Daq [m^2/s]	Daq' [m^2/s]	Daq$_{mean}$ [m^2/s]	STDEV [m^2/s]	Daq$_{ref}$ [m^2/s]
Benzene	48.47	26.01	0.5366	4.27	1053	1.60×10^{-9}	1.58×10^{-9}	1.12×10^{-9}	3.16×10^{-10}	$(9.40\text{-}11.60)\times10^{-10}$
Benzene	48.47	25.22	0.5204	4.27	1053	1.68×10^{-9}				
Benzene	48.47	27.64	0.5703	4.27	1053	1.45×10^{-9}				
Benzene	195.22	35.91	0.1839	17.92	1053	1.04×10^{-9}	1.04×10^{-9}			
Benzene	488.97	0.47	0.0010	75.08	1053	1.02×10^{-9}	1.02×10^{-9}			
Benzene	488.97	0.41	0.0008	104.13	927	8.48×10^{-10}	8.48×10^{-10}			
Toluene	18.87	9.88	0.5237	4.27	1053	1.66×10^{-9}	1.67×10^{-9}	1.06×10^{-9}	4.15×10^{-10}	$(8.34\text{-}9.70)\times10^{-10}$
Toluene	18.87	9.25	0.4903	4.27	1053	1.83×10^{-9}				
Toluene	18.87	10.50	0.5566	4.27	1053	1.51×10^{-9}				
Toluene	41.99	9.54	0.2272	17.92	1053	9.09×10^{-10}	9.09×10^{-10}			
Toluene	135.81	0.29	0.0021	75.08	1053	9.00×10^{-10}	9.00×10^{-10}			
Toluene	135.81	0.26	0.0019	104.13	927	7.49×10^{-10}	7.49×10^{-9}			
Ethylbenzene	5.76	2.91	0.5056	4.27	1053	1.76×10^{-10}	1.74×10^{-9}	1.04×10^{-9}	4.75×10^{-10}	$(7.85\text{-}9.20)\times10^{-10}$
Ethylbenzene	5.76	2.75	0.4778	4.27	1053	1.90×10^{-10}				
Ethylbenzene	5.76	3.12	0.5421	4.27	1053	1.58×10^{-10}				
Ethylbenzene	12.79	2.89	0.2256	17.92	1053	9.13×10^{-10}	9.13×10^{-10}			
Ethylbenzene	50.85	0.17	0.0034	75.08	1053	8.33×10^{-10}	8.33×10^{-10}			
Ethylbenzene	50.85	0.16	0.0032	104.13	927	6.90×10^{-10}	6.90×10^{10}			
BAM	360.65	291.17	0.8074	3.97	886	7.05×10^{-10}	6.62×10^{-10}	6.08×10^{-10}	5.08×10^{-11}	4.32×10^{-10}
BAM	360.65	298.92	0.8288	3.97	927	5.91×10^{-10}				
BAM	360.65	281.33	0.7801	3.97	1053	6.88×10^{-10}				
BAM	360.65	266.87	0.7400	6.00	886	6.56×10^{-10}	6.68×10^{-10}			
BAM	360.65	248.71	0.6896	6.00	1053	6.81×10^{-10}				
BAM	360.65	218.45	0.6057	9.90	886	6.62×10^{-10}	6.48×10^{-10}			
BAM	360.65	222.87	0.6180	9.90	927	6.08×10^{-10}				
BAM	360.65	196.29	0.5443	9.90	1053	6.76×10^{-10}				
BAM	360.65	89.36	0.2478	27.02	1053	5.68×10^{-10}	5.68×10^{-10}			
BAM	360.65	58.98	0.1636	40.26	886	5.88×10^{-10}	5.88×10^{-10}			
BAM	360.65	27.87	0.0773	59.38	927	5.39×10^{-10}	5.39×10^{-10}			
BAM	360.65	0.03	0.0001	104.00	1773	5.86×10^{-10}	5.86×10^{-10}			
Metolachlor	93.37	78.14	0.8369	3.97	886	5.87×10^{-10}	5.70×10^{-10}	5.02×10^{-10}	5.64×10^{-11}	$(4.82\text{-}5.16)\times10^{-10}$
Metolachlor	93.37	78.91	0.8451	3.97	927	5.30×10^{-10}				
Metolachlor	93.37	75.35	0.8070	3.97	1053	5.94×10^{-10}				
Metolachlor	93.37	72.92	0.7809	6.00	886	5.39×10^{-10}	5.61×10^{-10}			
Metolachlor	93.37	67.91	0.7273	6.00	1053	5.83×10^{-10}				

Metolachlor	93.37	61.93	0.6633	9.90	886	5.42×10^{-10}	5.36×10^{-10}
Metolachlor	93.37	62.99	0.6746	9.90	927	4.97×10^{-10}	
Metolachlor	93.37	55.93	0.5990	9.90	1053	5.69×10^{-10}	
Metolachlor	93.37	29.06	0.3113	27.02	1053	4.75×10^{-10}	4.75×10^{-10}
Metolachlor	93.37	21.36	0.2288	40.26	886	4.79×10^{-10}	4.79×10^{-10}
Metolachlor	93.37	13.11	0.1404	59.38	927	4.13×10^{-10}	4.13×10^{-10}
Metolachlor	93.37	0.05	0.0005	104.00	1773	4.77×10^{-10}	4.77×10^{-10}

Table S2 Estimation of the characteristic factor σ of each diffusion cell, with Cl^- as test solute*

No.cell	$C(0)$ [g/L]	$C(t)$ [g/L]	f [-]	time [h]	σ [cm^{-2}]	σ_{mean} [m^{-2}]	STDEV [m^{-2}]
new_1	3.52	3.07	0.87	22	0.08812	886	6.5
new_1	4.42	3.29	0.74	47	0.08903		
new_2	4.42	3.12	0.71	47	0.10503	1053	4.3
new_2	3.84	1.92	0.50	93	0.10563		
new_3	3.52	3.04	0.86	22	0.09444	927	25.3
new_3	4.42	3.27	0.74	47	0.09087		
new'_4	3.48	1.25	0.36	75.2	0.19305	1773	222.5
new'_4	3.35	1.59	0.48	65.3	0.16158		

* Test experiments were conducted with 0.1 mol/L KCl solution. $D_{aq\text{-}Cl^-} = 1.96 \times 10^{-9}$ m^2/s

Table S3 Measured D_{aq} of benzene, toluene, ethylbenzene, BAM and metolachlor

Compound	D_{aq}-measured [m^2/s]	D_{aq}-from literature [m^2/s]
Benzene	$11.2 \pm 3.2 \times 10^{-10}$*	$(9.40–11.60) \times 10^{-10}$ (6-8)
Toluene	$10.6 \pm 4.2 \times 10^{-10}$	$(8.34–9.70) \times 10^{-10}$ (6-8)
Ethylbenzene	$10.4 \pm 4.8 \times 10^{-10}$	$(7.85–9.20) \times 10^{-10}$ (7-9)
BAM	$6.08 \pm 0.51 \times 10^{-10}$	4.32×10^{-10} (10)
Metolachlor	$5.02 \pm 0.56 \times 10^{-10}$	$(4.82–5.16) \times 10^{-10}$ (7, 11)

*Uncertainties express standard deviations.

Table S4 Parameters for transport modeling

Symbol	Parameter	Values	Unit	References
Transport parameters				
$v_{(BAM, MET)}$	seepage velocity	1.25	[m s^{-1}]	experimental
$v_{(toluene)}$	seepage velocity	1.16	[m s^{-1}]	experimental
$d_{eff(BAM,MET)}$	effective grain size for classical equation	0.001	[m]	fitted
$d_{eff(BAM)-Chiogna}$	effective grain size for Chiogna et al. equation	0.0025	[m]	fitted
$d_{eff(toluene)}$	effective grain size for classical equation	0.0005	[m]	fitted
$\Phi_{(BAM, MET)}$	porosity	0.450	[-]	experimental
$\Phi_{(toluene)}$	porosity	0.434	[-]	experimental
$\alpha_{l(BAM, MET)}$	longitudinal dispersivity	6×10^{-4}	[m]	fitted
$\alpha_{l(toluene)}$	longitudinal dispersivity	2×10^{-4}	[m]	fitted
$\alpha_{t(BAM, MET)}$	transverse dispersivity	1.9×10^{-4}	[m]	$\alpha_t = d_{eff} \times 3/16$
$\alpha_{t(toluene)}$	transverse dispersivity	9.4×10^{-5}	[m]	$\alpha_t = d_{eff} \times 3/16$
D_{aq}^{BAM}	diffusion coefficient of BAM	6.08×10^{-10}	[m^2 s^{-1}]	diffusion experiment
D_{aq}^{MET}	diffusion coefficient of metolachlor	5.02×10^{-10}	[m^2 s^{-1}]	diffusion experiment
$D_{aq}^{toluene}$	diffusion coefficient of toluene	1.06×10^{-9}	[m^2 s^{-1}]	diffusion experiment
D_t^{BAM}	Transverse dispersion coefficient of BAM	2.99×10^{-9}	[m^2 s^{-1}]	$D_t = \alpha_t v + D_{aq}\Phi$
D_t^{MET}	Transverse dispersion coefficient of metolachlor	2.94×10^{-9}	[m^2 s^{-1}]	$D_t = \alpha_t v + D_{aq}\Phi$
$D_t^{Toluene}$	Transverse dispersion coefficient of toluene	1.72×10^{-9}	[m^2 s^{-1}]	$D_t = \alpha_t v + D_{aq}\Phi$
Inflow concentrations				
C_{in}^{BAM}	Inlet concentration of BAM	400	[mg L^{-1}]	experimental
C_{in}^{MET}	Inlet concentration of metolachlor	100	[mg L^{-1}]	experimental
$C_{in}^{Toluene}$	Inlet concentration of toluene	34.2	[mg L^{-1}]	experimental

Table S5 Summary of diffusion-induced isotope fractionation ε_{diff} and exponents of an assumed power law mass dependency of labelled organic compounds, noble gases and ions from literature.

Species	Heavy to light isotopes isotopologues	D_H/D_L	ε_{diff} [‰]	β [-]**	References
Labeled organic compounds					
Isopropyl alcohol	C_3D_7HO/C_3H_8O	0.993±0.006[a]	-7±6[a]	0.06±0.05[b]	LaBolle et al., 2008[12]
tert-Butyl alcohol	$C_4D_9HO/C_4H_{10}O$	0.997±0.002[a]	-3±2[a]	0.023±0.023[b]	LaBolle et al., 2008[12]
benzene	C_6D_6/C_6H_6	1.019±0.002[a]	19±2[a]	-0.247±0.026[a]	Rolle and Jin, 2017[6]
		1.000±0.005[c]	0±5[c]	0.0±0.1[b]	Kopinke et al., 2020[13]
		1.00±0.01[c]	0±10[c]	0.0±0.1[b]	Kopinke et al., 2018[14]*

cyclohyxane	C_6D_{12}/C_6H_{12}	1.00±0.01[c]	0±10[c]	0.0±0.1[b]	Kopinke et al., 2018[14]*
toluene	C_7D_8/C_7H_8	0.962±0.002[a]	-38±2[a]	0.46±0.02[a]	Rolle and Jin, 2017 [6]
		0.963±0.002[a]	-37±2[a]	0.455±0.023[a]	Jin et al., 2014[9]
		1.00±0.01[c]	0±10[c]	0.0±0.1[b]	Kopinke et al., 2018[14]*
		1.00±0.01[c]	0±10[c]	0.0±0.1[b]	Kopinke et al., 2020[13]
	$C_7D_5H_3/C_7H_8$	1.00±0.01[c]	0±10[c]	0.0±0.1[b]	Kopinke et al., 2018[14]*
ethylbenzene	C_8D_{10}/C_8H_{10}	0.960±0.02[a]	-40±2[a]	0.455±0.027[a]	Jin et al., 2014[9]
Noble gases					
He	$^4He/^3He$	0.87±0.03[d]	-130±30[d]	0.486±0.012[b]	Jahne et al., 1987[15]
Ne	$^{22}Ne^{20}Ne$	0.990±0.003[a]	-10±3[a]	0.104±0.032[b]	Tyroller et al., 2018[16]
	$^{23}Ne^{20}Ne$	0.9931±0.0008[e]	-6.9±0.8[e]	0.073±0.008[b]	Tempest and Emerson, 2013[17]*
Ar	$^{40}Ar/^{36}Ar$	0.948±0.004[a]	-52±4[a]	0.508±0.040[b]	Tyroller et al., 2014[18]
	$^{40}Ar/^{36}Ar$	0.9961±0.0003[e]	-3.90±0.3[e]	0.037±0.003[b]	Tempest and Emerson, 2013[17]*
	$^{40}Ar/^{36}Ar$	0.9963±0.0003[a]	-3.69±0.25[a]	0.035±0.002[b]	Seltzer et al., 2019[19]*
Kr	$^{84}Kr/^{82}Kr$	0.9995±0.0023[e]	-0.50±0.23[e]	0.021±0.050[b]	Tyroller et al., 2018[16]
	$^{84}Kr/^{82}Kr$	0.9995[g]	-0.50[g]	0.021[g]	Seltzer et al., 2019[19]*
	$^{86}Kr/^{82}Kr$	0.9986[g]	-1.40[g]	0.029[g]	Seltzer et al., 2019[19]*
	$^{84}Kr/^{83}Kr$	0.998±0.010[e]	-2±10[e]	0.200±0.423[b]	Tyroller et al., 2018[16]
	$^{86}Kr/^{84}Kr$	0.9965±0.0052[e]	-3.50±0.52[e]	0.149±0.111[b]	Tyroller et al., 2018[16]
Xe	$^{132}Xe/^{129}Xe$	1.0015±0.0025[e]	1.5±2.5[e]	-0.065±0.056[b]	Tyroller et al., 2018[16]
	$^{136}Xe/^{129}Xe$	0.9990[g]	-1.00[g]	0.019[g]	Seltzer et al., 2019[19]*
	$^{132}Xe/^{131}Xe$	0.9997±0.0012[e]	-0.3±1.2[e]	0.039±0.079[b]	Tyroller et al., 2018[16]
	$^{136}Xe/^{132}Xe$	0.9993±0.0020[e]	-0.7±2.0[e]	0.023±0.035[b]	Tyroller et al., 2018[16]
	$^{134}Xe/^{132}Xe$	1.0014±0.0018[e]	1.40±1.8[e]	-0.093±0.060[b]	Tyroller et al., 2018[16]
Ions					
Li	$^7Li/^6Li$	0.9965[g]	-3.5[g]	0.023[g]	Kunze and Fuoss, 1962[20]
	$^7Li/^6Li$	0.99772±0.00013[f]	-2.28±0.13[f]	0.015±0.001[b]	Richter et al., 2006[21]
	$^7Li/^6Li$	0.989±0.002[f]	-11±2[f]	0.071±0.010[b]	Fritz, 1992[22]
Na	$^{24}Na/^{22}Na$	0.998±0.002[a]	-2±2[a]	0.023±0.020[b]	Pikal, 1972[23]
Mg	$^{25}Mg/^{24}Mg$	1.00003±0.00003[f]	0.03±0.03[f]	0.0007±0.0007[b]	Richter et al., 2006[21]
K	$^{41}K/^{39}K$	0.9979[g]	-2.10[g]	0.042±0.002[j]	Bourg et al., 2010[24]
Ca	$^{44}Ca/^{40}Ca$	0.9997[g]	-0.43[g]	0.0045±0.0005[j]	Bourg et al., 2010[24]
Fe	$^{56}Fe/^{54}Fe$	0.99991±0.00002[i]	-0.09±0.02[i]	0.0024±0.0001[b]	Rodushkin et al., 2004[25]
Zn	$^{66}Zn/^{64}Zn$	0.9999±0.00001[i]	-0.06±0.01[i]	0.0019±0.0000[b]	Rodushkin et al., 2004[25]
Ba	$^{137}Ba/^{134}Ba$	0.99978[g]	-0.22[g]	0.010±0.002[h]	Van Zuilen et al., 2016[26]
Cl	$^{37}Cl/^{35}Cl$	0.99857±0.0004[f]	-1.43±0.04[f]	0.025±0.007[b]	Richter et al., 2006[21]
	$^{37}Cl/^{35}Cl$	0.99836±0.00020[a]	-1.64±0.20[a]	0.030±0.004[b]	Eggenkamp and Coleman, 2009[27]
Br	$^{81}Br/^{79}Br$	0.99920±0.00017[a]	-0.80±0.17[a]	0.032±0.007[b]	Eggenkamp and Coleman, 2009.[27]

[a] Published or calculated standard deviation based on the data in literature, [b] β uncertainty calculated according to Gauss' error propagation law by including the uncertainty of D_H/D_L, [c] published system uncertainty, [d] unclear uncertainty, [e] standard deviation recalculated based on published standard error, [f] standard deviation recalculated from reported 2 times standard deviation, [g] uncertainty not available, [h] estimated uncertainty range, [i] standard deviation of isotope ratio measurements, [j] uncertainty from linear regression.*Studies on mass transfer of species between two phases (water/gas phase[17, 19] or water/n-octane phase[14]).** β values were either the published values or recalculated based on eq 2.

References

1. Bauer, R. D.; Maloszewski, P.; Zhang, Y.; Meckenstock, R. U.; Griebler, C., Mixing-controlled biodegradation in a toluene plume--results from two-dimensional laboratory experiments. *J. Contam. Hydrol.* **2008,** *96* (1-4), 150-68.
2. Torrentó, C.; Bakkour, R.; Ryabenko, E.; Ponsin, V.; Prasuhn, V.; Hofstetter, T. B.; Elsner, M.; Hunkeler, D., Fate of four herbicides in an irrigated field cropped with corn: lysimeter experiments. *Procedia Earth Planet. Sci.* **2015,** *13*, 158-161.
3. Anneser, B.; Einsiedl, F.; Meckenstock, R. U.; Richters, L.; Wisotzky, F.; Griebler, C., High-resolution monitoring of biogeochemical gradients in a tar oil-contaminated aquifer. *Appl. Geochem.* **2008,** *23* (6), 1715-1730.
4. Ehrl, B. N.; Kundu, K.; Gharasoo, M.; Marozava, S.; Elsner, M., Rate-limiting mass transfer in micropollutant degradation revealed by isotope fractionation in chemostat. *Environ. Sci. Technol.* **2019,** *53* (3), 1197-1205.
5. Qiu, S.; Eckert, D.; Cirpka, O. A.; Huenniger, M.; Knappett, P.; Maloszewski, P.; Meckenstock, R. U.; Griebler, C.; Elsner, M., Direct experimental evidence of non-first order degradation kinetics and sorption-induced isotopic fractionation in a mesoscale aquifer: 13C/12C analysis of a transient toluene pulse. *Environ. Sci. Technol.* **2013,** *47* (13), 6892-9.
6. Rolle, M.; Jin, B., Normal and inverse diffusive isotope fractionation of deuterated toluene and benzene in aqueous systems. *Environ. Sci. Technol. Lett.* **2017,** *4* (7), 298-304.
7. EPA On-line Tools for Site Assessment Calculation. https://www3.epa.gov/ceampubl/learn2model/part-two/onsite/estdiffusion.html.
8. Rowe, R. K.; Mukunoki, T.; Sangam, H. P., BTEX diffusion and sorption for a geosynthetic clay liner at two temperatures. *J. Geotech. Geoenviron. Eng.* **2005,** *131* (10), 1211-1221.
9. Jin, B.; Rolle, M.; Li, T.; Haderlein, S. B., Diffusive fractionation of BTEX and chlorinated ethenes in aqueous solution: quantification of spatial isotope gradients. *Environ. Sci. Technol.* **2014,** *48* (11), 6141-50.
10. Jorgensen, P. R.; Klint, K. E.; Kistrup, J. P., Monitoring well interception with fractures in clayey till. *Ground Water* **2003,** *41* (6), 772-9.
11. Martínez, L.; Lechón, Y.; Sánchez-Brunete, C.; Tadeo, J. L., Persistence of metolachlor, atrazine and deethylatrazine in soil and its simulation by deterministic models. *Toxicol. Environ. Chem.* **1996,** *54* (1-4), 219-232.
12. LaBolle, E. M.; Fogg, G. E.; Eweis, J. B.; Gravner, J.; Leaist, D. G., Isotopic fractionation by diffusion in groundwater. *Water Resour. Res.* **2008,** *44* (7), W07405.
13. Kopinke, F.-D.; Georgi, A., H/D-isotope fractionation due to aqueous phase diffusion – Deuterated hydrocarbons revisited. *Chemosphere* **2020,** *258*, 127357.

14. Kopinke, F. D.; Georgi, A.; Roland, U., Isotope fractionation in phase-transfer processes under thermodynamic and kinetic control - Implications for diffusive fractionation in aqueous solution. *Sci. Total Environ.* **2018,** *610-611*, 495-502.
15. Jähne, B.; Heinz, G.; Dietrich, W., Measurement of the diffusion coefficients of sparingly soluble gases in water. *J. Geophys. Res.: Oceans* **1987,** *92* (C10), 10767-10776.
16. Tyroller, L.; Brennwald, M. S.; Busemann, H.; Maden, C.; Baur, H.; Kipfer, R., Negligible fractionation of Kr and Xe isotopes by molecular diffusion in water. *Earth Planet. Sci. Lett.* **2018,** *492*, 73-78.
17. Tempest, K. E.; Emerson, S., Kinetic isotopic fractionation of argon and neon during air–water gas transfer. *Mar. Chem.* **2013,** *153*, 39-47.
18. Tyroller, L.; Brennwald, M. S.; Mächler, L.; Livingstone, D. M.; Kipfer, R., Fractionation of Ne and Ar isotopes by molecular diffusion in water. *Geochim. Cosmochim. Acta* **2014,** *136*, 60-66.
19. Seltzer, A. M.; Ng, J.; Severinghaus, J. P., Precise determination of Ar, Kr and Xe isotopic fractionation due to diffusion and dissolution in fresh water. *Earth Planet. Sci. Lett.* **2019,** *514*, 156-165.
20. Kunze, R. W.; Fuoss, R. M., Conductance of the alkali Halides. III. The isotopic lithium chlorides. *J. Phys. Chem.* **1962,** *66* (5), 930-931.
21. Richter, F. M.; Mendybaev, R. A.; Christensen, J. N.; Hutcheon, I. D.; Williams, R. W.; Sturchio, N. C.; Beloso Jr, A. D., Kinetic isotopic fractionation during diffusion of ionic species in water. *Geochim. Cosmochim. Acta* **2006,** *70* (2), 277-289.
22. Fritz, S. J., Measuring the ratio of aqueous diffusion coefficients between 6Li+ Cl− and 7Li+ Cr− by osmometry. *Geochim. Cosmochim. Acta* **1992,** *56* (10), 3781-3789.
23. Pikal, M. J., Isotope effect in tracer diffusion. Comparison of the diffusion coefficients of 24Na+ and 22Na+ in aqueous electrolytes. *J. Phys. Chem.* **1972,** *76* (21), 3038-3040.
24. Bourg, I. C.; Richter, F. M.; Christensen, J. N.; Sposito, G., Isotopic mass dependence of metal cation diffusion coefficients in liquid water. *Geochim. Cosmochim. Acta* **2010,** *74* (8), 2249-2256.
25. Rodushkin, I.; Stenberg, A.; Andrén, H.; Malinovsky, D.; Baxter, D. C., Isotopic fractionation during diffusion of transition metal ions in solution. *Anal. Chem.* **2004,** *76* (7), 2148-2151.
26. van Zuilen, K.; Müller, T.; Nägler, T. F.; Dietzel, M.; Küsters, T., Experimental determination of barium isotope fractionation during diffusion and adsorption processes at low temperatures. *Geochim. Cosmochim. Acta* **2016,** *186*, 226-241.
27. Eggenkamp, H. G. M.; Coleman, M. L., The effect of aqueous diffusion on the fractionation of chlorine and bromine stable isotopes. *Geochim. Cosmochim. Acta* **2009,** *73* (12), 3539-3548.